

ORFS-agent: Tool-Using Agents for Chip Design Optimization

Amur Ghose, Andrew B. Kahng, Sayak Kundu, Zhiang Wang
 {aghose,abk,sakundu,zhw033}@ucsd.edu
 UC San Diego, La Jolla, California, USA

Abstract—Machine learning has been widely used to optimize complex engineering workflows across numerous domains. In the context of integrated circuit design, modern flows (e.g., going from a register-transfer level netlist to physical layouts) involve extensive configuration via thousands of parameters, and small changes to these parameters can have large downstream impacts on desired outcomes – namely design performance, power, and area. Recent advances in Large Language Models (LLMs) offer new opportunities for learning and reasoning within such high-dimensional optimization tasks. In this work, we introduce *ORFS-agent*, an LLM-based iterative optimization agent that automates parameter tuning in an open-source hardware design flow. *ORFS-agent* adaptively explores parameter configurations, demonstrating clear improvements over standard Bayesian optimization approaches in terms of resource efficiency and final design metrics. Our empirical evaluations on two different technology nodes and a range of circuit benchmarks indicate that *ORFS-agent* can improve both routed wirelength and effective clock period by over 13%, all while using 40% fewer optimization iterations. Moreover, by following natural language objectives to trade off certain metrics for others, *ORFS-agent* demonstrates a flexible and interpretable framework for multi-objective optimization. Crucially, *ORFS-agent* is modular and model-agnostic, and can be plugged in to any frontier LLM without any further fine-tuning.

Index Terms—Open-Source EDA, Physical Design, Autotuning, Large Language Model

I. INTRODUCTION

Large Language Models (LLMs) have reshaped AI, excelling at natural-language generation, question answering, and zero-/few-shot learning [7]. Their emergent reasoning spans mathematical problem solving, code generation, and multi-step orchestration via agent frameworks [12]. LLMs integrate into agent systems [53], combining API calls, predefined functions (“tool use”), and context windows to meet language-defined goals. Agents already serve a range of fields from healthcare to voice-controlled computing.

Research on LLMs has seen advances in neural architecture search [13] [33], combinatorial optimization [5] [38], and heuristic selection [6] [29], all of which are relevant to chip design tasks. Chip design relies on a complex EDA flow that turns high-level hardware descriptions into manufacturable layouts. Each stage exposes hundreds or thousands of hyperparameters (timing constraints, placement strategies, routing heuristics, etc.) whose joint settings strongly affect power, performance, and area (PPA). At advanced nodes, design complexity and the design flow parameter space balloon further [1].

The concrete problem. We target **LLM-driven black-box optimization** across varied objectives, circuits, and technology nodes. In ML terms, this is **context-based** Bayesian optimization: LLM agents exploit metadata (e.g., log files) as heuristics. Traditional Bayesian optimization (BO) can tune EDA parameters well, but pure black-box methods miss domain knowledge and need explicit objectives. By contrast, LLMs have broad “world knowledge” and can use chain-of-thought to iteratively propose and refine parameters [65] [56].

LLM agents interface with chip design tools, parse intermediate results, call domain APIs, and adjust flow parameters in a human-like loop. They can boost the efficiency of heuristic frameworks (e.g., BO).

Distinction from other works: fine-tuning vs. model-agnostic approaches. Many recent efforts apply domain-specific fine-tuning. ChatEDA [56], ChipNeMo [34], and JARVIS [43] curate EDA-centric corpora, retrain or instruction-tune a base model, and then self-host the resulting checkpoint; this entails recurring data-collection, training, and maintenance costs whenever a stronger foundation model is released.

ChatEDA, for instance, fine-tunes an open-source (or API-tunable) model on Q-A examples. Each new SOTA model demands another fine-tune: closed models (e.g., Claude) seldom allow this, and open models lag the frontier. Fine-tuning plus lifecycle management and hosting may cost USD \$10k, and the maintainer pays for inference.

Other methods avoid retraining, and instead wrap or retrieve around frozen SOTA models. EDA-Copilot [4], Ask-EDA [50], OpenROAD-Assistant [48], RAG for EDA-QA [45] and ORAssistant [26] combine retrieval-augmented generation with off-the-shelf models for tool-usage questions, while surveys [65] [63] [47] highlight the draw of lightweight, model-agnostic agents.

Our agent follows this latter paradigm: it wraps whatever SOTA model is available, with zero extra training cost; our full experiments can run on Grok-Mini for less than USD \$10. Further, while previous agents such as ChatEDA build general Q-A support for engineers, our agent focuses solely on optimizing flow parameters.

Our contributions. We develop **ORFS-agent**, an LLM-driven autotuner for an open-source chip-design flow that can surpass Bayesian optimization using fewer flow runs. Our main contributions are:

- We embed ORFS-agent in OpenROAD-flow-scripts (ORFS) [79]. It schedules parallel ORFS runs, reads intermediate metrics (wirelength, timing, power), and iteratively refines parameters to optimize post-route results. Leveraging ORFS’s METRICS2.1 logging [22], the agent skips bad configurations and gives robust, efficient chip design optimization. Modularity allows frictionless switching of models.
- ORFS-agent obeys natural-language instructions to weight or constrain design metrics (e.g., to favor timing over wirelength) and is able to leverage existing BO libraries inside its tool-use loop.
- On ASAP7 and SKY130HD (three circuits each), ORFS-agent trims ORFS calls and improves wirelength and effective clock period by $\geq 13\%$ over baseline, beating the BO-based ORFS AutoTuner [22].

In the following, Section II reviews BO and recent LLM-EDA work. Section III gives details of ORFS-agent – prompts, data, and iterations. Section IV gives experiments. Section V concludes and sketches future work. Our code is open-sourced at [80].

II. RELATED WORK

We taxonomize related work into three areas: Open-Source EDA, Bayesian Optimization, and LLMs for Optimization in EDA. Appendix A gives additional discussion of EDA flow and OpenROAD.

A. Open-Source EDA and OpenROAD as an ML Testbed

We target LLM/ML EDA research based on the permissively open-sourced **OpenROAD** [3], whose code, logs and data can be made public to enable reproducible training and evaluation. Tcl/Python APIs expose every flow stage for capture of live metrics and debug, which is vital for ML agents. With its RTL-to-GDSII scope, transparency and active community, OpenROAD provides a robust testbed. **ORFS** wraps OpenROAD in editable JSON/Tcl for large-scale experiments [79].

B. Bayesian Optimization in Flow Tuning

Bayesian optimization (BO) is a widely used approach for parameter autotuning in EDA flows [22], including in commercial tools such as Synopsys DSO.ai [75] and Cadence Cerebrus [70]. BO is efficient in terms of samples and solution space search, but has several drawbacks.

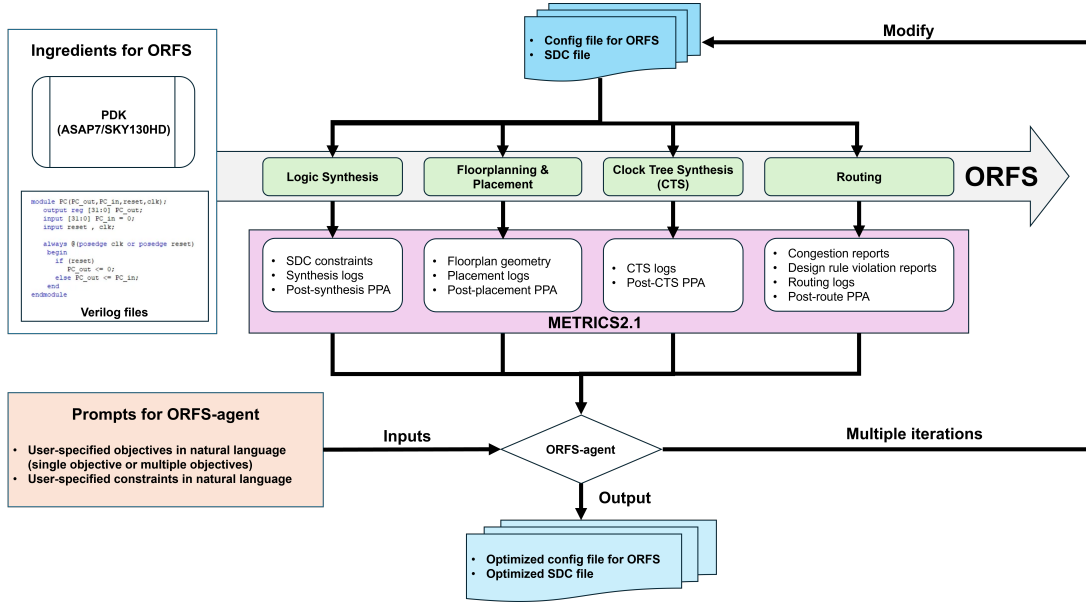


Fig. 1: ORFS-agent integrated with OpenROAD-flow-scripts (ORFS); metrics gathered via METRICS2.1 [22].

- *Contextual and knowledge limitations.* BO frameworks typically do not incorporate domain knowledge unless manually encoded (e.g., at PDK level). Further, they do not adapt from past results.
 - *Explicit objective functions.* BO frameworks require explicitly defined objective functions, possibly missing complex or subjective criteria. This can hinder effectively balancing PPA in chip design.
 - *Scalability challenges.* High-dimensional spaces and large designs can combinatorially overwhelm traditional BO approaches [60].
- We seek flexible, context-aware and data-driven approaches to parameter tuning. Large Language Models offer a promising foundation.

C. Large Language Models in EDA Optimization

LLMs such as GPT [7] absorb web- and paper-scale corpora, giving them broad technical knowledge. They parse design logs, infer context, and suggest EDA optimizations [54] [65] [56].

Contextual knowledge and adaptivity. Unlike black-box Bayesian optimization, LLMs ingest circuit data, retrieve literature, and adjust strategies on the fly. They read partial metrics (e.g., post-clock tree synthesis (-CTS) timing) and learn user preferences without explicit objectives [41].

Recent progress. Advisor systems LLM4EDA [65] and ChatEDA [56] guide placement and timing fixes. Startups Silogy [85], Silimate [84], Atopile [69], Diode Computers [74] and ChipAgents [71] extend AI across design tasks. New methods such as LLAMBO [32] [77] and works presented at ICLAD [76] and MLCAD [78] Symposia reinforce the trend. Multi-fidelity BO and meta-surrogates [14] [27] [49] improve sampling efficiency yet still treat flows as opaque; by contrast, LLMs promise context-aware tuning. Large-scale industrial adoption of LLMs for EDA can be seen, e.g., NVIDIA’s MARCO framework shows graph-based multi-agent task solving for design flows [72]. Open problems in LLM-based hardware verification are mapped in [57].

D. Working with LLMs and Agent Frameworks

LLMs require scaffolding beyond raw prompts. Techniques include:

- *Prompt engineering* crafts system/user messages for clarity.
- *Chain-of-thought* reasoning [54] elicits stepwise logic.
- *Retrieval-augmented generation* [30] injects external documents.
- *Tool-use/agent frameworks* [46] [15] [44] let an LLM call shells or solvers, parse error logs [20], and orchestrate full flows [28].

These methods enable adaptive, metric-driven tuning.

LLM agents for optimization. Agents excel at ill-specified goals [61], prompt search [16], hyperparameter tuning [35], autonomous research [19], and benchmark challenges [18]. EE Times has forecast the advent of collaborating AI agents for chip design by 2025 [11].

Coupling with Bayesian optimization. LLM-based agents can parse PPAC metrics, narrow BO search spaces, prune bad configs, or switch heuristics. Blending BO with symbolic reasoning [42] [52] yields targeted, adaptive flows. **ORFS-agent** builds on this foundation.

More modern advances. OPRO [61] treats the model itself as the optimizer. LLAMBO warm-starts BO with zero-shot hints [32]. ADO-LLM fuses analog priors with BO loops [62]. ChatEDA [56] and the newer EDAid [58] systems wire agents straight into complete RTL-to-GDSII flows. RL efforts such as AutoDMP [2] [10] and Google’s graph-placement policy [39] show tractability of end-to-end layout.

Tool-centric agent stacks. Browser agents such as WebArena [64] surf, click, and scrape constraints for downstream solvers. Terminal aides such as ShellGPT [82] and Devin [73] run `make`, `git`, and `yosys` on command, closing the loop between code and silicon. API routers such as ToolLLM [46], Gorilla [44], and OpenAgents [59] map natural-language tasks onto thousands of REST calls and plugins. AutoGPT [51]-style self-looping controllers review results and re-issue actions, while the AI-Scientist [83] pipeline shows how the same pattern can automate hypothesis, experiment, and paper generation. At code level, AlphaCode 2 [66] beats 85% of Codeforces competitors; RL-trained VeriSeek [36] and retrieval-guided logic synthesis agents [8] trim Verilog area-delay in minutes. Together, browser, tool, and terminal hooks turn LLMs into end-to-end optimization engines.

Our work explores how these engines might advance the state of the art in heuristics-driven applied optimization domains such as EDA.

III. PROPOSED METHODOLOGY

We now introduce the integration framework of our ORFS-agent with OpenROAD-flow-scripts (ORFS). We then present an explanation of a single iteration of the ORFS-agent loop.

A. Overview of ORFS-agent

ORFS-agent is an end-to-end agent framework designed to optimize OpenROAD-based chip design flows according to user-specified objectives and constraints. ORFS-agent leverages an LLM capable of performing internal text-based reasoning and invoking external *tools* (function-calling). Our approach supports parallel runs of ORFS, partial

metric gathering and various optimization strategies. Figure 1 shows the overall framework of ORFS-agent.

The inputs to ORFS-agent include process design kits (PDKs) for the target technology node, target circuits described in Verilog files, and user-defined prompts. PDKs are sets of files that provide process-related information needed for chip implementation. In this work, we use two technology nodes: SKY130HD [81] and ASAP7 [68]. The prompts define the objective function and constraints in natural language. The objective function in this work is formulated as

$$F = \sum_{i=1}^n \alpha_i f_i,$$

where each f_i is a design metric (e.g., routed wirelength, worst negative slack) and each α_i is a nonnegative real weight. This formulation allows optimization of either a single metric or a weighted combination of multiple metrics. Then, ORFS-agent iteratively modifies the configuration file (config.mk) for ORFS and SDC files to optimize the specified objectives. The ORFS configuration file defines adjustable parameters (knobs) for floorplanning, placement, clock tree synthesis and routing. The SDC file specifies timing constraints for the target design, such as clock period. The outputs of ORFS-agent are the optimized configuration file for ORFS and the optimized SDC file; together, these optimize the user-specified objectives under given constraints.

ORFS-agent relies on an LLM (e.g., GPT, Claude, Llama) that can (i) read and modify files and logs; (ii) optionally invoke external tools via function calling, i.e., specify argument values for pre-existing functions (e.g., Python functions); and (iii) propose new parameter values to improve the objective under given constraints. There is a key distinction between direct LLM use and the use of *LLM-based agents* with *function-calling* capabilities. In the function-calling paradigm, the LLM is given a goal (e.g., “write a function to compute a matrix eigendecomposition”) along with a list of *tools*, which are black-box functions the LLM can invoke to facilitate task completion. For example, a tool named **ISDIAGONALIZABLE** determines whether a matrix M is diagonalizable and returns a Boolean value. The tools used in ORFS-agent fall into the following three categories.

- **INSPECT tools** allow the agent to *inspect* the data collected so far without context-level manipulation.
 - **OPTIMIZE tools** allow the agent to *model* and *optimize* the data by a suitable model such as a Gaussian process.
 - **AGGLOM tools** allow the agent to *sub-select* from possible hyperparameters obtained from an **OPTIMIZE** tool.
- In the basic function-calling agent loop, at iteration t with context C_t , the agent performs the following up to K times:
- **Observe:** Load the ORFS configuration file and SDC file, execute ORFS, and examine the results of ORFS;
 - **Query:** Call tools from the provided list (up to M times) to gather information and update the context to C_{t+1} ; and
 - **Alter:** Modify ORFS config/SDC files based on C_{t+1} .

By iterating through these steps, the function-calling agent incrementally refines its solutions by using external tools.

B. Overall Iteration Structure with Example and Tool Usage

We describe **one** iteration of the ORFS-agent loop, which executes K parallel runs of OpenROAD-flow-scripts, with K being provided by the user. As shown in Figure 2, each iteration consists of the following steps: **RUN**, **READ**, **COLLATE**, **INSPECT**, **OPTIMIZE**, **AGGLOMERATE** (optional) and **ALTER**.

We maintain a **GLOBALCONTEXT** that collects relevant parameters and partial metrics across steps. The initialization of this **GLOBALCONTEXT** at the first iteration is also the LLM prompt; this initialization, along with procedures for update between iterations for **GLOBALCONTEXT**, is separately discussed in Appendix E. Let K denote the number of parallel runs per iteration, and let **TIMEOUT**

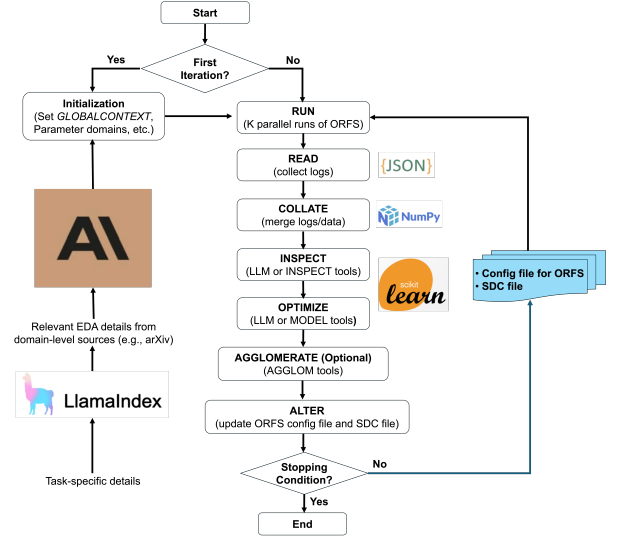


Fig. 2: Overall ORFS-agent flowchart.

specify the maximum runtime for each batch. Below, we show an example scenario with $K = 25$, **TIMEOUT** = 30 minutes and parameters (**Core Util**, **Clock Period**) that can be integrated, along with possible function-calling tools. Consider the j^{th} iteration. Assume that we target the **routed** wirelength and take the **CTS** wirelength as a surrogate (recalling that the CTS stage is earlier and thus likely does not time out).

Stage 1: RUN K Parallel Jobs. Launch K ORFS runs, each with distinct parameters, until the **TIMEOUT** is reached.

- **Example:** For $K = 25$ and **TIMEOUT** = 30 minutes, we launch 25 parallel runs, each exploring a different (**Core Util**, **Clock Period**) setting. All will run for at most 30 minutes, producing log files.
- **Tool use:** This set of runs might be derived from a previous iteration where **OPTIMIZE** or **AGGLOM** tools suggest new parameter sets.
- **No tool use:** If tool use is disabled, these parameter files arise from simple in-context operations.

Stage 2: READ. Gather JSON logs from the files generated by all **RUN** steps up to this iteration. These may contain partial surrogate metrics, e.g., from the CTS stage, or ground truth metrics from finished runs.

- **Example:** The agent collects $25 \times j$ JSON files, with routed wirelengths (ground truth) or earlier rough CTS wirelengths (surrogate).
- **No tools,** hence identical with or without tool use.

Stage 3: COLLATE. Merge the logs into a single dataset, storing outcomes for all $K \times j$ runs (e.g., a table or array).

- **Example:** Build a unified array with columns (**Core Util**, **Clock Period**, CTS wirelength, routed wirelength). The routed wirelength can be absent. If the CTS wirelength is absent, skip the row.
- **No tools,** hence identical with or without tool use.

Stage 4: INSPECT. Analyze the collated data.

- **Example:** For $\leq 25 \times j$ (\leq from skips) instances, find how **Clock Period** varies against the wirelength (actual target) and CTS wirelength (surrogate).

- **Tool use:** The agent calls pre-defined **INSPECT** tools to examine distributions; this allows sidestepping of in-context inspection of values. For example, **InspectDistribution**(**ARR**, **X**, **Y**, **Y_{surrogate}**) outputs the distributional relation between an input **X** and targets **Y** with surrogate targets **Y_{surrogate}**. Here we have **Clock Period** as **X**, CTS and routed wirelength as **Y_{surrogate}**, **Y** and **ARR** from the **COLLATE** step.

- **No tool use:** The agent reasons purely in context using its chain of thought by inspecting the data.

Stage 5: OPTIMIZE. Based on **INSPECT**, propose new parameter sets for the next iteration.

- *Example*: The agent calls an **OPTIMIZE** tool, e.g., a Gaussian process (GP) with the **COLLATE**-level data, to get 200 values of candidate **Clock Period**, **Core Util** pairs, using a **Matérn kernel**, and **Expected Improvement** as search strategy.
- *Tool use*: In general, we may have candidate points from **GP**(**ARR**, **args**, ...) or any other **OPTIMIZE** tool, obtaining many potential parameter sets. **ARR** arises from **collate**, and the agent decides on which **OPTIMIZE** tool to use, i.e., whether to use a Gaussian process at all, as well as the choice of **args** depending on what it finds at the **INSPECT** phase. This may include choices over the kernel used, selection algorithm, and so on.
- *No tool use*: The agent solely uses its own context to directly suggest a set of parameters.

Stage 6: AGGLOMERATE (optional). If more than K candidates are generated in the **OPTIMIZE** phase, then reduce to exactly K , e.g., by maximizing diversity or coverage.

- *Example*: Since the **GP** produces 200 new (**Core Util**, **Clock Period**) pairs; we sub-select to 25 via a valid **AGGLOM** tool, **EntropySelect**(**ARR**, **quality**, **points**). This function returns **points**, i.e., 25 pairs of (**Core Util**, **Clock Period**) that are considered set-level optimal with respect to the provided **quality** metric (wavelength improvement) on the same **ARR** from **COLLATE**.
- *Tool use*: The agent may use any number of **AGGLOM** tool choices from the LLM’s decisions along with parameters to call them with. The final output is of shape $K \times$ the number of parameters optimized.
- *No tool use*: Here, the **OPTIMIZE** case uses structured outputs to yield exactly K sets of parameter choices in context directly, and this **step is skipped**.

Stage 7: ALTER. Update ORFS configuration files with the newly selected parameter sets for the next iteration.

- *Example*: Generate 25 updated config/SDC files or commands, each having one of the chosen (**Core Util**, **Clock Period**) combinations.
- *No tools*, hence identical with or without tool use.

This process repeats until the stopping criteria – generally, total serial iteration count – are met. The outputs of stages **READ** through **AGGLOMERATE** enter the context window of ORFS-agent in each iteration, but do not necessarily enter the **GLOBALCONTEXT**. Context management and tool-level details are given in Appendix E.

IV. EXPERIMENTS AND RESULTS

Our experiments use six design instances comprising three circuits (IBEX, AES and JPEG) in two technology nodes (SKY130HD and ASAP7). All experiments are performed on a Google Cloud Platform (GCP) virtual machine with 112 virtual CPUs (C2D AMD Milan) and 220GB RAM. The flow is based on the ce8d36a commit of the OpenROAD-flow-scripts repository [79], along with associated versions of OpenROAD, KLayout, Yosys, and other dependencies.

Although the timeout to run depends on the circuit, each “iteration” is consistently defined as 25 parallel runs, with the exception of the JPEG circuits, which are run with 12 parallel runs each. Each of these parallel runs uses four vCPUs and 4 GB of RAM. These parallel runs write to different intermediate folders for logs and results, running Yosys and other steps in parallel without reusing intermediate steps. At the end of each iteration, a clean operation moves the logs and folders to a separate directory to avoid contamination.

Our experiments cover two settings. The first, “4-variable” setting involves optimizing over four parameters: **Core Utilization**, **TNS End Percent**, **LB Add On Place Density**, and **Clock Period**. The first three are in the configuration files of the respective circuits; Clock Period is in the SDC file. The second, “12-variable” setting has eight additional tunable parameters that guide the physical design flow more comprehensively. We distinguish three experimental cases.

- **4-variable, no tool use**, where the LLM optimizes over four variables solely through prompt-tuning and in-context learning;

Tech	Circuit	WL Optimization		ECP Optimization		Co-Optimization	
		WL	ECP*	ECP	WL*	WL**	ECP**
OR-AutoTuner Performance: 375 Iterations, 4 Parameters							
SKY130HD	IBEX	632918	14.52	10.17	811265	802786	10.49
	AES	514342	7.28	4.08	639876	564188	4.43
	JPEG	1263740	8.25	6.77	1421110	1304829	7.24
ASAP7	IBEX	104622	1510	1252	109346	107821	1264
	AES	68943	1634	431	78152	72303	446
	JPEG	269721	1172	950	284539	276453	978
Average		1.00	1.00	1.00	1.00	1.00	1.00
OR-AutoTuner Performance: 1000 Iterations, 12 Parameters							
SKY130HD	IBEX	630598	14.08	10.09	767451	750769	10.10
	AES	423730	5.02	3.81	563264	495781	3.89
	JPEG	1070038	7.77	6.57	1295066	1089166	7.29
ASAP7	IBEX	96086	3244	1188	103081	100837	1192
	AES	66934	2220	430	77067	71086	443
	JPEG	260683	1130	882	279621	273649	885
Average		0.92	1.18	0.96	0.94	0.93	0.95

TABLE I: **OR-AutoTuner results**. **Top block**: 375 iterations with 4 parameters. **Bottom block**: 1000 iterations with 12 parameters. Columns are grouped by optimization: *WL*-only (*WL*, *ECP**), *ECP*-only (*ECP*, *WL**), and co-optimization (*WL***, *ECP***). Bold font indicates superior results relative to Table II in the corresponding comparison class of (375, 4) or (600, 12) iterations and parameters.

- **4-variable with tool use**, where Bayesian optimization enhances performance; and
- **12-variable with tool use**, which incorporates all 12 variables along with the Bayesian optimization tools.

Our experimental choices reflect the LLM requiring more complex tools to tackle higher-dimensional optimization problems. All experiments involve either 375 (4-variable setting) or 600 iterations (12-variable setting). The ORFS-agent parameters are configured as follows: (i) the model is *claude-3-5-sonnet-20241022*; ¹ (ii) temperature is 0.1; (iii) nucleus and top-K sampling are disabled; and (iv) to always output $25 \times 4/12$ parameters (the number of parameters the LLM is optimizing over) in the specified format, we utilize JSON Mode (Structured Outputs API).² Appendix B provides additional experimental details.

The ORFS-agent is tasked with optimizing two specific figures of merit: the post-route **effective clock period** (*ECP*) and **routed wavelength** (*WL*).³ Due to potential timeouts during execution, these metrics may not always be available. Therefore, ORFS-agent also records the corresponding metrics from the earlier clock tree synthesis (CTS) stage of the flow.⁴ While our primary objective is to optimize either *ECP* or *WL*, we also track the **instance area**, **instance count**, **total power** and a derived metric called **PDP** ($PDP = \text{power} \times ECP$). Throughout this work, we adopt the following notations.

- *ECP** (resp. *WL**) denotes the value of *ECP* (resp. *WL*) when *WL* (resp. *ECP*) is optimized as the objective; and
- *ECP*** and *WL*** represent the values obtained when both metrics are jointly optimized in a multi-objective setting.

We use OR-AutoTuner as the baseline. We run OR-AutoTuner for 1000 iterations with 12 parameters to optimize, and for 375 iterations with 4 parameters to optimize. Results are shown in Table I.

In the following, Section IV-A presents results for single-objective optimization. Then, Subsection IV-B gives results for multi-objective optimization. We then demonstrate ORFS-agent’s capability to perform constrained optimization guided by natural language commands. Appendix C provides additional ablation studies for the ASAP7-IBEX

¹We do not observe any performance gains from the *o1*-class of models.

²In terms of API costs, all of our experiments, including all failed runs, cost US \$48. Claude Sonnet 3.5 has since been overtaken by models which are simultaneously better and cheaper by 5 – 10 \times per token. As noted above, approaches such as ChatEDA require fine-tuning, which costs significantly more (by at least 10–20 \times) and requires inference costs for serving the custom model.

³The unit of *ECP* is *ns* in SKY130HD and *ps* in ASAP7; routed wavelength is in μm ; power is in *W*; and area is in μm^2 .

⁴*WL'* denotes the estimated wavelength at the end of CTS.

Tech	Circuit	WL Optimization		ECP Optimization		Co-Optimization	
		WL	ECP*	ECP	WL*	WL**	ECP**
375 Iterations, 4 Parameters without Tool Use							
SKY130HD	IBEX	732793	11.47	10.82	815984	792947	11.00
	AES	531721	5.33	4.07	651219	637490	4.08
	JPEG	1257231	7.28	6.69	1371607	1344380	6.77
ASAP7	IBEX	106044	1324	1281	113854	114576	1287
	AES	70955	446	430	72427	71644	440
	JPEG	277654	1084	1016	289031	286142	1069
Average		1.04	0.75	1.02	1.00	1.04	1.00
375 Iterations, 4 Parameters with Tool Use							
SKY130HD	IBEX	726874	10.91	10.74	752566	736275	10.84
	AES	526782	5.12	4.02	601492	572966	4.06
	JPEG	1268544	7.08	6.64	132785	1302494	6.74
ASAP7	IBEX	101788	1298	1242	112788	106854	1254
	AES	70288	448	435	72144	71422	442
	JPEG	270184	968	952	283544	273126	958
Average		1.03	0.71	1.00	0.82	0.98	0.97
600 Iterations, 12 Parameters with Tool Use							
SKY130HD	IBEX	657091	12.25	10.42	721099	706087	11.06
	AES	483426	4.82	3.96	539878	500296	4.06
	JPEG	1237829	6.94	6.54	1308171	1254030	6.62
ASAP7	IBEX	97305	1278	1248	105562	102205	1260
	AES	69824	456	432	74582	71084	438
	JPEG	270963	905	878	275944	271822	882
Average		0.98	0.71	0.98	0.92	0.94	0.96

TABLE II: **ORFS-agent** results for various tuning settings. **Top:** 375 iterations, 4 parameters (no tool); **Middle:** 375 iterations, 4 parameters (with tool); **Bottom:** 600 iterations, 12 parameters (with tool). Each row reports the figures of merit under WL-only, ECP-only, and Co-optimization objectives. Bold font indicates superior results relative to Table I in the corresponding comparison class of (375, 4) or (1000, 12) iterations and parameters.

design. Studies on data leakage, model confidence and robustness are presented in Appendix D.

A. Single-objective Optimization

In the single-objective optimization scenario (e.g., minimizing routed wirelength WL), the LLM agent receives an additional natural language instruction appended to its prompt. Specifically, the instruction is:

There is only a single objective to optimize in this problem. You observe that the value inside the final JSON is WL , while the corresponding baseline value is WL_α . Your effective loss to minimize should be $\frac{WL}{WL_\alpha}$.

where WL_α denotes the routed wirelength obtained using the default configuration of OpenROAD-flow-scripts and serves as a fixed baseline for normalization.⁵

However, due to runtime timeouts, typically occurring during the detailed routing stage, the routed wirelength WL may not always be available. In contrast, the estimated wirelength at the end of CTS WL' almost always exists. If WL is absent but WL' exists, we include the following instruction:

You do not observe the correct value WL , but you observe a strong surrogate WL' , which you should use as a signal. Your effective loss should be $\frac{WL'}{WL_\alpha}$.

where WL'_α denotes post-CTS wirelength obtained under the same default configuration. This surrogate-based guidance enables the LLM to continue learning from partial information while maintaining alignment with the optimization objective.

The experimental results are shown in Table II. Before discussing these results, we would like to highlight that our results are obtained with the Claude 3.5 class of models. The very recent release of Sonnet 4 [67] has allowed us to check our experiments on a stronger model, and showcase the modularity afforded by ORFS-agent. With no fine-tuning needed, early results show substantial improvements – e.g., for ASAP7-IBEX (12-parameter case with tool use) a wirelength of **86397** μm is obtained by ORFS-agent using Sonnet 4 in less than 100 iterations. This is significantly better than what is achieved by either

ORFS-agent with Claude 3.5 or OR-AutoTuner. Appendix G gives further details.

With respect to Table II, key observations are as follows.

- **Comparison between default ORFS and ORFS-agent:** ORFS-agent (600 iterations, 12 parameters with tool use) achieves an average improvement of 13.2% in wirelength (or ECP) when configured for wirelength (or ECP) optimization.
- **Comparison between OR-AutoTuner and ORFS-agent:** Despite using 40% fewer iterations, ORFS-agent (600 iterations, 12 parameters, with tool use) achieves better results than OR-AutoTuner on 12 out of 24 metrics measured for single-objective optimization, thereby exactly drawing on cases of superiority.
- **Impact of tool use** (375 iterations and 4 parameters): ORFS-agent with tool use dominates ORFS-agent without tool use in 5 out of 6 cases, for both wirelength and effective clock period optimization.
- We notice that ORFS-agent does **not** significantly worsen the metric not being optimized. For instance, when optimizing wirelength on ASAP7-IBEX, the ECP obtained by ORFS-agent (600 iterations, 12 parameters with tool use) is 40% of that obtained by OR-AutoTuner. We hypothesize this is from the ECP values entering the agent's context window, causing it to avoid actions that would worsen ECP .

B. Multi-objective Optimization

In the case of multiple losses – e.g., WL and ECP – we instruct the LLM to consider the loss:

$$\frac{WL}{WL_\alpha} + \frac{ECP}{ECP_\alpha} \quad (1)$$

with the same substitution, if applicable, for ECP' , WL' if any of these are unavailable, with the same phrasing adopted above. The experimental results are shown in Table II. Key results are as follows.

- **Sustained gains.** Unlike single-objective optimization, where gains observed exceed 13%, gains on multi-objective cases are roughly 11.3% on ECP and 10.5% on wirelength simultaneously. This is measured relative to the baselines discussed in subsection IV-C, having 12 parameters to optimize for 600 iterations with tool use. Out of 12 comparisons to OR-AutoTuner, ORFS-agent is superior in 6 of them, thereby exactly drawing.
- **No worsening.** As with single-objective optimization, ORFS-agent does not worsen any metric – either ECP or wirelength, relative to baselines. In fact, both QoR metrics improve **simultaneously**.

We visualize the optimization trajectory of instance count alongside wirelength and ECP in Figure 3. We notice that instance count can actually *improve for free*. To better understand gains on auxiliary metrics (metrics that do not directly enter the optimization function), we examine correlational properties of metrics in Figure 4. We look at how other metrics vary in an optimization run as we carry out ORFS-level runs for ASAP7-IBEX under different parameters and differing optimization goals – namely wirelength, ECP , or a combination of

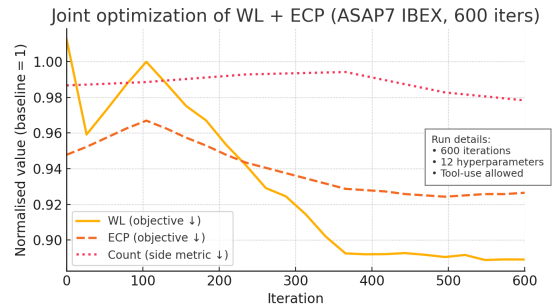


Fig. 3: Optimization trajectory of ASAP7-IBEX (co-optimization, 600 iterations, 12 parameters with tool use). Wirelength (WL), effective clock period (ECP), and instance count (Count) are normalized to baseline values from default ORFS settings.

⁵The baseline results obtained using the default configuration of OpenROAD-flow-scripts are shown in Section IV-C.

the two as defined above. Some metrics do not “come for free” – *ECP* and power, for instance, have an inverse relationship with each other.

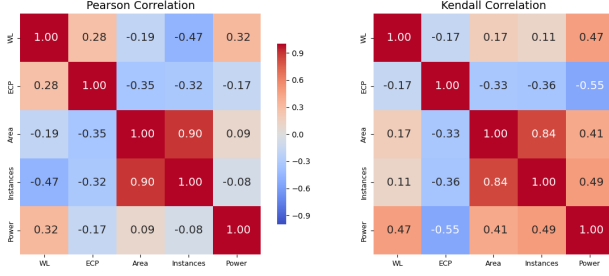


Fig. 4: Correlation of metrics for ASAP7-IBEX: wirelength (*WL*), effective clock period (*ECP*), instance area (*Area*), instance count (*Instances*) and power (*Power*). Pearson correlation captures linear relationships; Kendall correlation captures rank-based relationships.

C. Baseline Comparisons

We obtain baseline solution metrics using the default ORFS flow parameters seen at the cited commit hash. These metrics are shown in Tables III and IV. Compared to these baselines, ORFS-agent achieves an improvement of over 13% versus the default ORFS flow parameters, when averaged across all six testcases and single-metric (i.e., *ECP* and *WL*) comparisons. (For all metrics, **lower** is better.) For additional context, Table V gives post-route metrics obtained by a proprietary, closed-source tool on ASAP7 circuits; these are quoted from [21].

	CTSWL (<i>WL</i> ¹)	CTSECP (<i>ECP</i> ¹)	<i>WL</i>	<i>ECP</i>
SKY130HD-IBEX	550963	10.84	808423	11.54
ASAP7-IBEX	93005	1308	115285	1361
SKY130HD-AES	428916	5.34	589825	4.72
ASAP7-AES	61103	432	75438	460
SKY130HD-JPEG	1199090	8.00	1374966	7.73
ASAP7-JPEG	266510	1096	300326	1148

TABLE III: Metric values for default ORFS results.

	Instance area	Count	Power	PDP
SKY130HD-IBEX	192784	20944	0.097	1.12
ASAP7-IBEX	2729	21831	0.057	77.58
SKY130HD-AES	122361	18324	0.411	1.94
ASAP7-AES	2046	17693	0.149	68.54
SKY130HD-JPEG	541327	65670	0.811	6.27
ASAP7-JPEG	7904	68287	0.138	158.42

TABLE IV: Derived values for default ORFS results.

Design	Tool	<i>ECP</i>	Area	Power
AES	Comm	582	40679	0.3498
	ORFS*	697	58995	0.2361
IBEX	Comm	1123	68843	0.7949
	ORFS*	1654	47969	0.4739
JPEG	Comm	616	156700	0.7522
	ORFS*	899	182624	0.7944

TABLE V: Results for AES, IBEX, and JPEG on optimized OpenROAD (ORFS*) and proprietary tools (Comm) as cited from [21].

D. Constrained Optimization under Natural Language Commands

A human engineer often has goals that differ from the utility functions used by OR-AutoTuner. For example, a human might be instructed: “Optimize metric *X* as much as possible, while not allowing metrics *A, B, C* to deteriorate by more than 2%.” This percentage value is with reference to the previously mentioned baseline values in Tables III and IV. This form of constrained optimization is generally not straightforward with existing OR-AutoTuner setups. LLMs can attempt such optimization by incorporating these constraints directly into their context. We study this phenomenon in Table VI, where we optimize *ECP* and *WL* subject to a maximum worsening of 2% and 4% in other metrics of interest – Area, Instance Count, Power, and PDP. We term the maximum worsening allowed as “leeway”.

We observe that this often improves **multiple** metrics *simultaneously*. This avoids the problem of, e.g., worsening power values observed in Figure 4. Comparisons to OR-AutoTuner and further discussion are given in Appendix C, along with tests for robustness and prompt-level sensitivity (Appendix D). ORFS-agent respects the constraints (in terms of maximum 2% or 4% worsening) imposed. Simultaneously, it improves the metrics targeted for optimization, relative to baseline values.

4 parameters and no tools				
Metric	WL Optimization		ECP Optimization	
	2% leeway	4% leeway	2% leeway	4% leeway
WL	-8.18%	-8.51%	-7.62%	-6.34%
ECP	-1.07%	2.51%	-2.98%	-3.06%
Area	-1.36%	-1.68%	-1.18%	-0.80%
Count	-1.55%	-1.70%	-1.35%	-1.17%
PDP	-2.03%	-9.04%	-5.12%	-0.05%
Power	-0.97%	-11.27%	-2.20%	3.11%
12 parameters with tools				
Metric	WL Optimization		ECP Optimization	
	2% leeway	4% leeway	2% leeway	4% leeway
WL	-11.24%	-12.05%	-7.9%	-8.3%
ECP	-3.02%	-2.12%	-4.18%	-4.46%
Area	-2.17%	-1.92%	-1.12%	0.56%
Count	-1.62%	-1.74%	-1.31%	-1.06%
PDP	-3.25%	-0.27%	-6.88%	-0.77%
Power	-0.24%	1.87%	-2.81%	3.86%

TABLE VI: Constrained optimization results. **Red positive numbers** indicate worsening, i.e., an increase relative to baseline; “leeway” indicates the maximum worsening allowed.

V. CONCLUSION AND FUTURE DIRECTIONS

In this work, we propose ORFS-agent, a plug-in open-source framework that integrates LLMs into OpenROAD for hyperparameter optimization. Despite using 40% fewer iterations, ORFS-agent achieves results comparable to OR-AutoTuner. ORFS-agent adopts a modular, provider-agnostic framework, which makes it user-friendly and easy to adopt. ORFS-agent can switch seamlessly among LLM providers (e.g., Anthropic, OpenAI, Gemini) without reconfiguration. Additionally, ORFS-agent avoids the cost and complexity of fine-tuning and deployment, and requires no retraining or infrastructure changes when a new LLM is released. Thus, our ORFS-agent can instantly benefit from model breakthroughs. For example, our preliminary results with Claude 4 Sonnet models (released May 22, 2025) already surpass both Claude 3.5-based ORFS-agent and OR-AutoTuner. Unlike fine-tuning-based approaches, ORFS-agent can rapidly and cost-effectively adopt stronger models, making it both competitive and appealing.

Our future work will explore the following directions. (i) The field has seen the emergence of reasoning-based models, which use a longer chain of thought process before making decisions. These reasoning-based models are then fine-tuned to task-specific agentic models. We aim to integrate such agentic models into ORFS-agent to enhance its decision-making depth and adaptability. (ii) Our current framework uses a fixed set of pre-defined tools. In future work, we will enable the LLM agent to generate its own tools dynamically, which avoids the hand-coding of specific tools and increases flexibility in handling different circuits and technology nodes. (iii) We plan to integrate ORFS-agent with search APIs and RAG tools that enable the agent to access documentation, literature or previous published results. And (iv) we will evaluate ORFS-agent on larger-scale circuits and with more hyperparameters to assess its scalability and robustness. In combination with open-sourcing and OpenROAD integration, we believe that this work will add to the foundations for new research on LLMs for physical design and EDA.

ACKNOWLEDGMENTS

This work is partially supported by the Samsung AI Center.

REFERENCES

- [1] A. Agnesina, K. Chang and S. K. Lim, "Parameter Optimization of VLSI Placement Through Deep Reinforcement Learning," *TCAD*, 42 (4) (2022), pp. 1295–1308.
- [2] A. Agnesina, P. Rajvanshi, T. Yang, G. Pradipta, A. Jiao, B. Keller et al., "AutoDMP: Automated DREAMPlace-based Macro Placement," *Proc. ISPD*, 2023, pp. 149–157.
- [3] T. Ajayi, D. Blaauw, T.-B. Chan, C.-K. Cheng, V. A. Chhabria, D. K. Choo, et al., "OpenROAD: Toward a Self-Driving, Open-Source Digital Layout Implementation Tool Chain," *Proc. Gov. Microcircuit Applications and Critical Technology Conf.*, 2019, pp. 1105–1110.
- [4] Z. Xiao, X. He, H. Wu, B. Yu and Y. Guo, "EDA-Copilot: A RAG-Powered Intelligent Assistant for EDA Tools," *TODAES* (2025).
- [5] Y. Bengio, A. Lodi and A. Prouvost, "Machine Learning for Combinatorial Optimization: A Methodological Tour d'Horizon," *Eur. J. Oper. Res.*, 290 (2) (2021), pp. 405–421.
- [6] E. K. Burke, M. Gendreau, M. Hyde, G. Kendall, G. Ochoa, E. Özcan and R. Qu, "Hyper-Heuristics: A Survey of the State of the Art," *J. Oper. Res. Soc.*, 64 (12) (2013), pp. 1695–1724.
- [7] T. B. Brown, B. Mann, N. Ryder, M. Subbiah, J. Kaplan and P. Dhariwal et al., "Language Models Are Few-Shot Learners," *Advances in Neural Information Processing Systems*, 33 (2020), pp. 1877–1901.
- [8] A. B. Chowdhury, M. Romanelli, B. Tan, R. Karri and S. Garg, "Retrieval-Guided Reinforcement Learning for Boolean Circuit Minimization," *Proc. ICLR*, 2024.
- [9] M. Chen, J. Tworek, H. Jun, Q. Yuan, H. P. de Oliveira Pinto and J. Kaplan et al., "Evaluating Large Language Models Trained on Code," *arXiv preprint arXiv:2107.03374*, 2021.
- [10] C.-K. Cheng, A. B. Kahng, S. Kundu, Y. Wang and Z. Wang, "Assessment of Reinforcement Learning for Macro Placement," *Proc. ISPD*, 2023, pp. 158–166.
- [11] N. Dahad, "AI Agents Will Work With AI Agents for Chip Design in 2025," *EE Times*, 20 Dec. 2024.
- [12] I. Drori, S. Zhang, R. Shuttlesworth, L. Tang, A. Lu and E. Ke et al., "A Neural Network Solves, Explains, and Generates University Math Problems by Program Synthesis and Few-Shot Learning at Human Level," *arXiv preprint arXiv:2112.15594*, 2022.
- [13] T. Elsken, J. H. Metzen and F. Hutter, "Neural Architecture Search: A Survey," *J. Mach. Learn. Res.*, 20 (55) (2019), pp. 1–91.
- [14] S. Falkner, A. Klein and F. Hutter, "BOHB: Robust and Efficient Hyperparameter Optimization at Scale," *Proc. ICML*, 2018, pp. 1437–1446.
- [15] Y. Ge, W. Hua, K. Mei, J. Ji, J. Tan and S. Xu et al., "OpenAGI: When LLM Meets Domain Experts," *arXiv preprint arXiv:2304.04370*, 2023.
- [16] Q. Guo, R. Wang, J. Guo, B. Li, K. Song, X. Tan et al., "Connecting Large Language Models With Evolutionary Algorithms Yields Powerful Prompt Optimizers," *arXiv preprint arXiv:2309.08532*, 2023.
- [17] S. Hooker, "The Hardware Lottery," *arXiv preprint arXiv:2009.06489*, 2020.
- [18] Q. Huang, J. Vora, P. Liang and J. Leskovec, "Benchmarking Large Language Models as AI Research Agents," *Advances in Neural Information Processing Systems*, 2023.
- [19] T. Ifargan, L. Hafner, M. Kern, O. Alcalay and R. Kishony, "Autonomous LLM-Driven Research—From Data to Human-Verifiable Research Papers," *NEJM AI*, 2 (1) (2025), pp. A10a2400555.
- [20] C. E. Jimenez, J. Yang, A. Wettig, S. Yao, K. Pei, O. Press and K. Narasimhan, "SWE-bench: Can Language Models Resolve Real-World GitHub Issues?," *arXiv preprint arXiv:2310.06770*, 2023.
- [21] J. Jung, A. B. Kahng, S. Kundu, Z. Wang and D. Yoon, "IEEE CEDA DATC Emerging Foundations in IC Physical Design and MLCAD Research," *Proc. ICCAD*, 2023, pp. 1–7.
- [22] J. Jung, A. B. Kahng, S. Kim and R. Varadarajan, "METRICS2.1 and Flow Tuning in the IEEE CEDA Robust Design Flow and OpenROAD," *Proc. ICCAD*, 2021, pp. 1–9.
- [23] A. B. Kahng, J. Lienig, I. L. Markov and J. Hu, "VLSI Physical Design: From Graph Partitioning to Timing Closure," Springer, 2011.
- [24] A. B. Kahng, "Machine Learning Applications in Physical Design: Recent Results and Directions," *Proc. ISPD*, 2018, pp. 68–73.
- [25] A. B. Kahng, "A Mixed Open-Source and Proprietary EDA Commons for Education and Prototyping," *Proc. ICCAD*, 2022, pp. 1–6.
- [26] A. Kaintura, P. R., S. L. and I. I. Almeida, "ORAssistant: A Custom RAG-Based Conversational Assistant for OpenROAD," *arXiv preprint arXiv:2410.03845*, 2024.
- [27] K. Kandasamy, G. Dasarathy, J. B. Oliva, J. Schneider and B. Póczos, "Multi-Fidelity Bayesian Optimisation With Continuous Approximations," *Proc. ICML*, 2017, pp. 1799–1808.
- [28] O. Khatib, A. Singhi, P. Maheshwari, Z. Zhang, K. Santhanam and S. Vardhaman et al., "DSPy: Compiling Declarative Language Model Calls Into Self-Improving Pipelines," *arXiv preprint arXiv:2310.03714*, 2023.
- [29] L. Kotthoff, "Algorithm Selection for Combinatorial Search Problems: A Survey," *Data Mining and Constraint Programming*, Springer, 2016, pp. 149–190.
- [30] P. Lewis, E. Perez, A. Piktus, F. Petroni, V. Karpukhin and N. Goyal et al., "Retrieval-Augmented Generation for Knowledge-Intensive NLP Tasks," *Advances in Neural Information Processing Systems*, 33 (2020), pp. 9459–9474.
- [31] Y. Lin, S. Dhar, W. Li, H. Ren, B. Khailany and D. Z. Pan, "DREAMPlace: Deep Learning Toolkit-Enabled GPU Acceleration for Modern VLSI Placement," *Proc. DAC*, 2019, pp. 1–6.
- [32] T. Liu, N. Astorga, N. Seedat and M. van der Schaar, "Large Language Models to Enhance Bayesian Optimization," *arXiv preprint arXiv:2402.03921*, 2024.
- [33] H. Liu, K. Simonyan and Y. Yang, "DARTS: Differentiable Architecture Search," *arXiv preprint arXiv:1806.09055*, 2018.
- [34] M. Liu, T.-D. Ene, R. Kirby, C. Cheng, N. Pinckney, R. Liang et al., "ChipNeMo: Domain-Adapted LLMs for Chip Design," *arXiv preprint arXiv:2311.00176*, 2024.
- [35] S. Liu, C. Gao and Y. Li, "Large Language Model Agent for Hyper-Parameter Optimization," *arXiv preprint arXiv:2402.01881*, 2024.
- [36] M. Liu, N. R. Pinckney, B. Khailany and H. Ren, "VeriSeek: Reinforcement Learning With Golden Code Feedback for Verilog Generation," *arXiv preprint arXiv:2407.18271*, 2024.
- [37] Y.-C. Lu, J. Lee, A. Agnesina, K. Samadi, and S. K. Lim, "GAN-CTS: a Generative Adversarial Framework for Clock Tree Prediction and Optimization," *Proc. ICCAD*, 2019, pp. 1–8.
- [38] N. Mazyavkina, S. Sviridov, S. Ivanov and E. Burnaev, "Reinforcement Learning for Combinatorial Optimization: A Survey," *Comput. & Oper. Res.*, 134 (2021), p. 105400.
- [39] A. Mirhoseini, A. Goldie, M. Yazgan, J. W. Jiang, E. Songhori, S. Wang et al., "A Graph Placement Methodology for Fast Chip Design," *Nature*, 594 (2021), pp. 207–212.
- [40] A. Mishchenko, S. Chatterjee and R. Brayton, "DAG-Aware AIG Rewriting: A Fresh Look at Combinational Logic Synthesis," *Proc. DAC*, 2006, pp. 532–535.
- [41] L. Ouyang, J. Wu, X. Jiang, D. Almeida, C. Wainwright and P. Mishkin et al., "Training Language Models to Follow Instructions With Human Feedback," *Advances in Neural Information Processing Systems*, 35 (2022), pp. 27730–27744.
- [42] L. Pan, A. Albalak, X. Wang and W. Yang, "Logic-LM: Empowering Large Language Models With Symbolic Solvers for Faithful Logical Reasoning," *arXiv preprint arXiv:2305.12295*, 2023.
- [43] G. Pasandi, K. Kunal, V. Tej, K. Shan, H. Sun, S. Jain et al., "JARVIS: A Multi-Agent Code Assistant for High-Quality EDA Script Generation," *arXiv preprint arXiv:2505.14978*, 2025.
- [44] S. G. Patil, T. Zhang, X. Wang and J. E. Gonzalez, "Gorilla: Large Language Model Connected With Massive APIs," *arXiv preprint arXiv:2305.15334*, 2023.
- [45] Y. Pu, Z. He, T. Qiu, H. Wu, and B. Yu, "Customized Retrieval Augmented Generation and Benchmarking for EDA Tool Documentation QA," *Proc. ICCAD*, 2024, pp. 1–9.
- [46] Y. Qin, S. Liang, Y. Ye, K. Zhu, L. Yan and Y. Lu et al., "ToolLLM: Facilitating Large Language Models to Master 16,000+ Real-World APIs," *arXiv preprint arXiv:2307.16789*, 2023.
- [47] N. Rai, "Enhancing Electronic Design Automation With Large Language Models: A Taxonomy, Analysis and Opportunities," *TechRxiv preprint*, 2025.
- [48] U. Sharma, B.-Y. Wu, S. R. D. Kankipati, V. A. Chhabria, and A. Rovinski, "OpenROAD-Assistant: An Open-Source Large Language Model for Physical Design Tasks," *Proc. MLCAD*, pp. 1–7, 2024.
- [49] R. Shu, J. Wang and W. Li, "MetaBO: Meta-Learning for Fast Bayesian Optimization in Chip Design," *TCAD*, 2024, Early Access.
- [50] L. Shi, M. Kazda, B. Sears, N. Shropshire and R. Puri, "Ask-EDA: A Design Assistant Empowered With LLM, Hybrid RAG and Abbreviation De-Hallucination," *arXiv preprint arXiv:2406.06575*, 2024.
- [51] G. Sung, "AI Agents: AutoGPT Architecture & Breakdown," *Medium*, 2023, <https://medium.com/@georgesung/ai-agents-autogpt-architecture-breakdown-ba37d60db944>.
- [52] T. H. Trinh, Y. Wu, Q. V. Le, H. He and T. Luong, "Solving Olympiad Geometry Without Human Demonstrations," *Nature*, 625 (7995) (2024), pp. 476–482.
- [53] L. Wang, C. Ma, X. Feng, Z. Zhang, H. Yang, J. Zhang et al., "A Survey on Large Language Model Based Autonomous Agents," *Frontiers of Computer Science*, 18 (6) (2024), p. 186345.
- [54] J. Wei, X. Wang, D. Schuurmans, M. Bosma, B. Ichter and F. Xia et al., "Chain-of-Thought Prompting Elicits Reasoning in Large Language Models," *arXiv preprint arXiv:2201.11903*, 2022.
- [55] N. H. E. Weste and D. M. Harris, "CMOS VLSI Design: A Circuits and Systems Perspective," Addison-Wesley, 2011.

- [56] H. Wu, Z. He, X. Zhang, X. Yao, S. Zheng, H. Zheng and B. Yu, "ChatEDA: A Large Language Model-Powered Autonomous Agent for EDA," *TCAD*, 2024.
- [57] Y.-H. Wu, Y. Lee and E. Lee, "Hardware Design and Verification With Large Language Models," *Electronics*, 14 (1) (2024), pp. 120.
- [58] H. Wu, H. Zheng, Z. He and B. Yu, "Divergent Thoughts Toward One Goal: LLM-Based Multi-Agent Collaboration System for Electronic Design Automation," *arXiv preprint arXiv:2502.10857*, 2025.
- [59] T. Xie, F. Zhou, Z. Cheng, C. Xiong and T. Yu, "OpenAgents: An Open Platform for Language Agents in the Wild," *arXiv preprint arXiv:2310.10634*, 2023.
- [60] L. Xu, F. Hutter, H. H. Hoos and K. Leyton-Brown, "SATzilla: Portfolio-Based Algorithm Selection for SAT," *J. Artif. Intell. Res.*, 32 (2008), pp. 565–606.
- [61] C. Yang, X. Wang, Y. Lu, H. Liu, Q. V. Le, D. Zhou and X. Chen, "Large Language Models as Optimizers," *arXiv preprint arXiv:2309.03409*, 2023.
- [62] Y. Yin, Y. Wang, B. Xu and P. Li, "ADO-LLM: Analog Design Bayesian Optimization With In-Context Learning of Large Language Models," *Proc. ICCAD*, 2024.
- [63] Z. He and B. Yu, "Large Language Models for EDA: Future or Mirage?," *Proc. ISPD*, 2024.
- [64] S. Zhou, F. F. Xu, H. Zhu and G. Neubig, "WebArena: A Realistic Web Environment for Building Autonomous Agents," *Proc. ICLR*, 2024.
- [65] R. Zhong, X. Du, S. Kai, Z. Tang, S. Xu and H.-L. Zhen et al., "LLM4EDA: Emerging Progress in Large Language Models for Electronic Design Automation," *arXiv preprint arXiv:2401.12224v1*, 2023.
- [66] "AlphaCode 2," TechCrunch coverage, 2023, <https://techcrunch.com/2023/12/06/deepmind-unveils-alphacode-2-powered-by-gemini/>.
- [67] Anthropic, "Introducing Claude 4," <https://www.anthropic.com/news/claude-4>.
- [68] ASAP7 PDK and Cell Libraries Repo. <https://github.com/The-OpenROAD-Project/asap7>
- [69] Atopile <https://www.atopile.io/>.
- [70] "Cerebrus," Cadence Intelligent Chip Explorer, https://www.cadence.com/en_US/home/tools/digital-design-and-signoff/soc-implementation-and-floorplanning/cerebrus-intelligent-chip-explorer.html.
- [71] ChipAgents <https://chipagents.ai/>.
- [72] "Configurable Graph-Based Task Solving With the MARCO Multi-AI Agent Framework for Chip Design," NVIDIA Developer Blog, 2025, <https://developer.nvidia.com/>.
- [73] "Devin: The First AI Software Engineer," Cognition Labs, 2024, <https://devin.ai>.
- [74] Diode Computers <https://www.ycombinator.com/companies/diode-computers-inc>.
- [75] "DSO.ai," Synopsys, <https://www.synopsys.com/ai/ai-powered-eda/dso-ai.html>.
- [76] ISLAD <https://www.islad.org/>.
- [77] "LLAMBO," <https://github.com/tennisonliu/LLAMBO>.
- [78] MLCAD <https://mlcad.org/symposium/2025/>.
- [79] "OpenROAD-Flow-Scripts," <https://github.com/The-OpenROAD-Project/OpenROAD-flow-scripts>, commit hash: ce8d36a.
- [80] "ORFS-Agent Code," <https://github.com/ABKGroup/ORFS-Agent>.
- [81] "SkyWater Open Source PDK," <https://github.com/google/skywater-pdk>.
- [82] "ShellGPT: A Command-Line Productivity Tool Powered by GPT-4," GitHub repository, 2023, https://github.com/TheR1D/shell_gpt.
- [83] "The AI Scientist: Towards Fully Automated Open-Ended Scientific Discovery," Project page, 2024, <https://sakana.ai/ai-scientist/>.
- [84] Silimate, <https://www.silimate.com/>.
- [85] Silogy, <https://www.ycombinator.com/companies/silogy>.

APPENDIX A EDA FLOW AND OPENROAD

The EDA flow is highly iterative, and suboptimal outcomes at one step may require going back to earlier steps for re-optimization (e.g., re-synthesizing the gate-level netlist or adjusting the placement). Each step generates logs and metrics that can be integrated into ML pipelines to guide subsequent decisions.

To systematically study LLM- and ML-driven EDA optimizations, we focus on the *OpenROAD* project [3]. In contrast to commercial EDA offerings, OpenROAD is fully open-source, thus avoiding copyright restrictions and enabling access to the internal details of its place-and-route algorithms, log files, and data structures. This open access allows the researchers to replicate and extend experiments, train and evaluate new models, and publish results without encountering proprietary barriers. [25]

In our work, leveraging OpenROAD allows us to (i) faithfully represent the full digital implementation flow (floorplanning, placement, clock tree synthesis, routing, etc.), (ii) integrate with a community-driven research ecosystem, and (iii) avoid opaque “black-box” workflows that impede effective ML experimentation. In particular, we are able to explore the potential of LLM-based EDA agents that can dynamically interpret intermediate results and fine-tune the flow for improved outcomes.

APPENDIX B ADDITIONAL EXPERIMENTAL DETAILS

A. Parameters, Metrics Tracked, and Surrogates

Table VII gives details of optimization parameters. The **Clock Period** is specified to one decimal place, and has no upper bound. **Core Utilization** and **TNS End Percent** are integers between 0 and 100 inclusive, while **LB Add On Place Density** (henceforth **LB Add On**) is a real number between 0 and 1, specified to two decimal places.

Parameter	Description	Type	Range
Clock Period	Target clock period (ns/ps)	Float	(0, ∞)
Core Utilization	% core utilization	Integer	[20, 99]
TNS End Percent	% violating endpoints to fix	Integer	[0, 100]
Global Padding	Global placement padding level	Integer	[0, 3]
Detail Padding	Detailed placement padding level	Integer	[0, 3]
Enable DPO	Detailed placement optimization	Binary	{0, 1}
Pin Layer Adjust	Routing adjust for metal2/3	Float	[0.2, 0.7]
Above Layer Adjust	Routing adjust for metal4 and above	Float	[0.2, 0.7]
Density Margin Add-On	Global density margin increase	Float	[0.00, 0.99]
Flatten Hierarchy	Flatten design hierarchy	Binary	{0, 1}
CTS Cluster Size	Number of sinks per CTS cluster	Integer	[10, 40]
CTS Cluster Diameter	Physical span of each CTS cluster	Integer	[80, 120]

TABLE VII: Overview of optimization parameters for both 4- and 12-parameter tuning. The top four rows form the 4-parameter case.

Optimized Metrics	
<i>ECP</i>	Final stage effective clock period, defined as the clock period minus the worst slack at the final stage of the build process.
<i>WL</i>	Post-detailed-routing wirelength.
Surrogates of Optimized Metrics	
<i>CTSECP (ECP')</i>	Effective clock period calculated at CTS
<i>CTSWL (WL')</i>	Estimated wirelength at CTS
Other Desirable Figures of Merit	
Instance Area	Total area of instances at the end of the optimization process
Instance Count	Number of instances at the end of the optimization process
EPC (PDP)	Energy per clock cycle equal to Power-Delay Product (PDP)
Power	Power consumption at the end of the optimization process

TABLE VIII: Definitions of key metrics.

Table VIII summarizes metrics tracked along with surrogates. The **Effective Clock Period** is defined as the **Clock Period** minus the worst slack at the finish stage. The metrics in Table VIII, along with their CTS-level surrogates and other desirable figures of merit, are based on the METRICS2.1 suite. The *Optimized metrics* directly enter the

natural language optimization process for the LLM. The *Surrogates* are included only if the primary metrics are unavailable due to timeouts. The remaining parameters – **Instance Area**, **Instance Count**, **PDP**, **Power** – are not directly optimized but are tracked as meaningful quantities. The expanded “12-variable setting” configuration adds the following eight tunable parameters that more comprehensively guide the physical design flow.

- **GP Pad:** Cell padding added during global placement to ensure sufficient spacing.
- **DP Pad:** Refinement of cell spacing in detailed placement for higher-quality placement.
- **DPO Enable:** A binary toggle for detailed placement optimization.
- **Pin Layer Adjust:** Routing resource adjustment on metal2 and metal3 layers.
- **Above Layer Adjust:** Similar routing resource adjustment for metal4 and higher layers.
- **Flatten:** A binary toggle that flattens design hierarchy.
- **CTS Cluster Size:** Target number of sinks grouped in each clock tree cluster.
- **CTS Cluster Diameter:** Target physical span of each clock tree cluster.

APPENDIX C ANALYSES AND ABLATIONS WITH ASAP7-IBEX

Effects of iterations and indirect optimization. We consider the results of the joint *WL*, *ECP* optimization as a function of the total serial iterations (keeping the number of parallel runs fixed at 25). The results are shown in Table IX, along with the other relevant figures of merit from Table VIII. Note that each row represents a separate run that is executed up to the corresponding number of serial iterations with 25 parallel runs. E.g., 5 should be considered as a total of $25 \times 5 = 125$ OpenROAD calls.

	<i>WL</i>	<i>ECP</i>	Area	Count	PDP	Power
5	108267	1353	2711	21614	78.474	0.058
10	108530	1334	2701	21529	73.37	0.055
15	111557	1294	2742	21875	89.286	0.069
20	110776	1293	2735	21831	89.217	0.069
25	112495	1298	2729	21796	85.734	0.066
30	108409	1328	2711	21614	77.024	0.058

TABLE IX: Optimization trajectory with 5 to 30 iterations, no tool use, 4-parameter setting.

This phenomenon can be well understood in the light of the **strong inter-correlations** of the data, presented in the main text (Subsection IV-B).

Reversibility. Table IX, indicates that optimizing wirelength and *ECP* jointly also optimizes other parameters. We also reverse this, and analyze the effect on wirelength and *ECP* when any one of these other parameters is optimized individually. The results of this process are presented in Table X. Notably, outcomes are *asymmetric* in that we see noticeably worse *ECP* outcomes, but with significantly lower power consumption.

	Count	Area	PDP	Power	<i>WL</i>	<i>ECP</i>
Count	21419	2679	68.632	0.046	109084	1492
Area	21437	2674	70.952	0.049	117411	1448
PDP	21432	2686	68.310	0.046	106070	1485
Power	21516	2689	68.540	0.046	107350	1490
<i>WL</i>	21540	2701	76.828	0.058	106044	1324
<i>ECP</i>	21799	2748	86.483	0.067	113854	1281

TABLE X: Results of optimizing the row-level objective on column-level outcomes: ASAP7-IBEX, no tool use, and 4-parameter setting.

To confirm that our results are consistent across tool use choices, we replicate this experiment using ASAP7-IBEX with 12 parameters and tool use enabled; results are presented in Table XI.

	Count	Area	PDP	Power	WL	ECP
Count	21356	2683	75.28	0.054	112984	1394
Area	21382	2642	76.21	0.058	120811	1314
PDP	21486	2706	59.41	0.047	107822	1264
Power	21416	2683	59.06	0.046	104622	1284
WL	21682	2672	99.68	0.078	97305	1278
ECP	21674	2684	102.34	0.082	105562	1248

TABLE XI: Results of optimizing the row-level objective on column-level outcomes: ASAP7-IBEX, tool use, and 12-parameter setting.

Constrained optimization under natural language commands.

We have presented the results of the constrained optimization setup in Subsection IV-D of the main text. Here, we continue on this vein. A human engineer is typically given commands significantly different from the utility functions used by OR-AutoTuner. Specifically, a common class of optimization commands relayed to humans takes the form:

“Optimize metric X as much as possible, while not allowing metrics A, B, C to deteriorate by more than 2%.”

This form of constrained optimization is generally not straightforward with existing OR-AutoTuner setups. LLMs can attempt such optimization by incorporating these constraints directly into their context. We study this phenomenon in Table XII and compare it to what OR-AutoTuner does in Tables XIII and XIV, where we optimize ECP and WL subject to a maximum worsening of 2% and 4% in other metrics of interest, i.e., Area, Instance Count, Power, and PDP. These percentage values are **always** with respect to the baseline values generated from default OR-AutoTuner parameters.

4 parameters and no tools				
Metric	WL Optimization		ECP Optimization	
	2% leeway	4% leeway	2% leeway	4% leeway
WL	-8.18%	-8.51%	-7.62%	-6.34%
ECP	-1.07%	2.51%	-2.98%	-3.06%
Area	-1.36%	-1.68%	-1.18%	-0.80%
Count	-1.55%	-1.70%	-1.35%	-1.17%
PDP	-2.03%	-9.04%	-5.12%	-0.05%
Power	-0.97%	-11.27%	-2.20%	3.11%
12 parameters with tools				
Metric	WL Optimization		ECP Optimization	
	2% leeway	4% leeway	2% leeway	4% leeway
WL	-11.24%	-12.05%	-7.9%	-8.3%
ECP	-3.02%	-2.12%	-4.18%	-4.46%
Area	-2.17%	-1.92%	-1.12%	0.56%
Count	-1.62%	-1.74%	-1.31%	-1.06%
PDP	-3.25%	-0.27%	-6.88%	-0.77%
Power	-0.24%	1.87%	-2.81%	3.86%

TABLE XII: Constrained optimization results. **Red positive numbers** indicate worsening, i.e., an increase relative to baseline; “leeway” indicates the maximum worsening allowed.

Metric	WL Optimization		ECP Optimization	
	2% leeway	4% leeway	2% leeway	4% leeway
WL	-9.03%	-5.69%	-3.23%	-1.41%
ECP	1.40%	1.03%	-1.31%	-2.60%
Area	-1.59%	-1.22%	-0.39%	-0.08%
Count	-1.80%	-1.71%	0.58%	-0.02%
PDP	-4.16%	-7.87%	-0.55%	-0.06%
Power	-5.49%	-8.81%	0.77%	2.61%

TABLE XIII: Constrained optimization results for OR-AutoTuner with 375 iterations, four parameters. **Red positive numbers** indicate worsening, i.e., an increase relative to baseline; “leeway” indicates the maximum worsening allowed.

The 4% tolerance case naturally gives rise to a Pareto frontier scatterplot of ECP versus WL , which is shown in Figure 5.

Metric	WL Optimization		ECP Optimization	
	2% leeway	4% leeway	2% leeway	4% leeway
WL	-12.53%	-9.26%	1.59%	-7.04%
ECP	1.07%	2.46%	-0.46%	-2.67%
Area	-1.86%	-1.65%	-0.49%	-1.95%
Count	-2.0%	-1.47%	0.16%	-1.57%
PDP	-7.17%	-4.17%	-1.10%	-2.31%
Power	-8.15%	-6.47%	-0.65%	0.37%

TABLE XIV: Constrained optimization results for OR-AutoTuner with 1000 iterations, 12 parameters. **Red positive numbers** indicate worsening, i.e., an increase relative to baseline; “leeway” indicates the maximum worsening allowed.

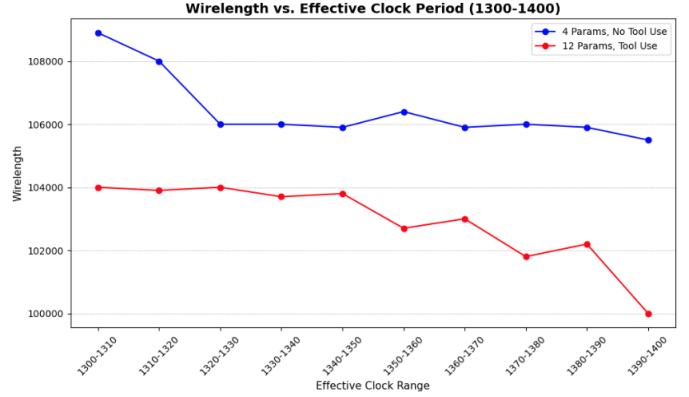


Fig. 5: Pareto frontier of ECP vs. WL under 4% tolerance, relative to the baseline. The blue line represents the case with 4 parameters and no tool use, and the red line represents the case with 12 parameters and tool use.

APPENDIX D

ABLATIONS FOR DATA LEAKAGE, CONFIDENCE AND ROBUSTNESS

In this appendix, we analyze statistical significance in Table XV, and study prompt-level ablations in Tables XVI and XVII. Table XVI presents outcomes of separate ablations of PDK (i.e., platform), circuit, and parameters. We refer readers to the implementation codebase [80] to understand the nature of this metadata. It can be clearly seen that the median values reflect the conclusions in Section IV and Section V of the main body of the paper, and that the interquartile ranges are small enough relative to the median to allow some assurances as to robustness.

Table XVII shows additional ablations, where “role” refers to the role of an EDA expert that the LLM is asked to pose as.

Metric	5 th	25 th	Median	75 th	95 th	Reported
WL	99820	98512	97360	96075	94980	97305
ECP*	1335	1301	1275	1251	1223	1278
ECP	1294	1271	1246	1224	1197	1248
WL*	108430	107180	105598	104125	102470	105562
WL**	105230	103720	102178	10162	99740	102205
ECP**	1311	1283	1259	1232	1201	1260

TABLE XV: Statistical significance over 20 independent ORFS-agent runs on the ASAP7-IBEX circuit. Percentile columns report the k^{th} worst value ($k=1, 5, 10, 15, 19$) among the 20 outcomes; “Reported” is the single-run value quoted in Section IV of the main paper.

Over the course of our work, the large amount of data from Anthropic naturally raises concerns about whether the LLM is simply caching or memorizing what it observes. This includes the possibility of interactions with other OpenROAD users who may be testing Claude models on similar outputs. We test these concerns in the following ways.

Circuit obfuscation. To assess potential memorization, we obfuscate the name of the ASAP7-IBEX circuit and subject it to the same iteration

Configuration	WL	ECP^*	ECP	WL^*	WL^{**}	ECP^{**}
Baseline	97305	1278	1248	105562	102205	1260
No PDK	99874	1385	1296	107284	105210	1275
No circuit	98743	1368	1301	106938	104782	1280
Both removed	106044	1324	1281	113854	114576	1287

TABLE XVI: Ablation on domain-knowledge content in prompts for ASAP7-IBEX. “No PDK” removes technology-node details; “No circuit” removes design-specific details; “Both removed” drops both. Higher WL/ECP indicate worse quality of result.

Prompt variant	WL	ECP^*	ECP	WL^*	WL^{**}	ECP^{**}
Baseline	97305	1278	1248	105562	102205	1260
No role	98044	1292	1255	106114	102934	1267
Blank params	99130	1310	1270	107039	103848	1278

TABLE XVII: Sensitivity of ORFS-agent to prompt simplifications on ASAP7-IBEX. “No role” deletes the system-role description; “Blank param” deletes parameter-guidance text.

vs. performance ablation test. The circuit name is changed to `obfs`, while the design platform input to the ORFS-agent remains ASAP7. Additionally, configuration settings are modified to rename the top-level module from “IBEX” to `obfs`. The ORFS-agent is also restricted from grepping log outputs that refer to the original name or netlist identifiers. Results are given in Tables XVIII and XIX.

	WL	ECP	Area	Count	PDP	Power
5	110605	1311	2731	21728	86.526	0.066
10	113186	1304	2741	21972	89.976	0.069
15	110358	1296	2735	21735	88.128	0.068
20	111918	1281	2746	21854	89.670	0.070
25	110965	1283	2733	21732	85.961	0.067
30	112645	1273	2746	21882	90.383	0.071

TABLE XVIII: Obfuscated results for ASAP7-IBEX, no tools, 4 parameters.

	WL	ECP	Area	Count	PDP	Power
5	114861	1316	2716	22015	84.22	0.064
10	105788	1294	2728	21986	90.58	0.070
15	106724	1286	2735	21924	87.45	0.068
20	106245	1278	2704	21864	84.35	0.066
25	103871	1276	2694	21882	90.60	0.071
30	103244	1272	2711	218008	94.13	0.074

TABLE XIX: Obfuscated results for ASAP7-IBEX, with tools, 12 parameters.

Statistical significance. We run the ASAP7-IBEX optimization for ECP , WL 10 times, with results given in Tables XX and XXI. Each individual row indicates the outcome with the lowest ECP in the final 25 iterations of an individual run. Even the worst of the 10 produces a result that is superior to OR-AutoTuner in terms of ECP .

	WL	ECP	Area	Count	PDP	Power
Run 1	116479	1290	2744	21781	90.300	0.070
Run 2	110232	1286	2736	21775	90.020	0.070
Run 3	121092	1287	2778	22181	91.377	0.071
Run 4	114576	1287	2746	22013	84.942	0.066
Run 5	109107	1303	2720	21636	80.786	0.062
Run 6	111054	1275	2740	21816	91.800	0.072
Run 7	116722	1279	2758	22098	89.530	0.070
Run 8	115933	1281	2766	21918	90.951	0.071
Run 9	109230	1309	2724	21656	82.467	0.063
Run 10	109342	1299	2728	21734	88.332	0.068

TABLE XX: 10-fold runs, ASAP7-IBEX, no tools, 4 parameters.

Robustness testing. We perform two layers of robustness testing. First, we add noise to every measurement: we multiply every observation O , at random, with the variable $1 + X_O$, where each X_O is an i.i.d. uniform random variable drawn from $[-0.05, 0.05]$. Next, we consider the scenario where our specification of the surrogate has

	WL	ECP	Area	Count	PDP	Power
Run 1	102289	1288	2726	21688	100.464	0.078
Run 2	102677	1285	2715	21722	102.800	0.080
Run 3	104200	1254	2705	21782	102.828	0.082
Run 4	103384	1270	2674	22092	109.220	0.086
Run 5	104922	1268	2678	21954	84.956	0.067
Run 6	102874	1269	2691	21894	91.368	0.072
Run 7	103982	1289	2712	21866	95.386	0.074
Run 8	103581	1275	2732	21895	96.900	0.076
Run 9	106742	1248	2725	21906	88.608	0.071
Run 10	105864	1252	2698	21967	87.640	0.070

TABLE XXI: 10-fold runs, ASAP7-IBEX, with tools, 12 parameters.

gone astray (i.e., the objective being optimized does not track what is desired. For this, we change all the CTS-level observations to be multiplied by $1 + X_{CTS}$, where X_{CTS} is an i.i.d. uniform random variable drawn from $[-0.2, 0.2]$. The results for ASAP7-IBEX are presented in Table XXII.

Run	WL	CP	Area	Count	PDP	Power
Overall perturbation, per objective case						
WL	104427	1318	2741	21782	92.26	0.070
ECP	106872	1268	2708	21905	98.90	0.078
$WL \& ECP$	107848	1274	2685	21802	96.82	0.076
CTS perturbation, per objective case						
WL	106898	1305	2673	21917	93.96	0.072
ECP	112824	1272	2711	21904	96.67	0.076
$WL \& ECP$	109873	1281	2705	21877	93.51	0.073

TABLE XXII: Perturbed runs, with tools, 12 parameters.

APPENDIX E

GLOBAL CONTEXT, INITIALIZATION, AND THE TOOLBOX

The **FunctionalORFS-agent** maintains a `GLOBALCONTEXT` containing the design environment details (PDK, circuit, task specifics, etc.). Each LLM call in the pipeline includes this global context, plus the relevant logs and data extracted at runtime. The `GLOBALCONTEXT` is initialized as the *prompt*, defined below.

LLM calls made within each part of an iteration – i.e., **INSPECT**, etc. – add the `LOCALCONTEXT` of that particular iteration. However, they are not necessarily passed on to the `GLOBALCONTEXT`. As we move from iteration j to iteration $j + 1$, `GLOBALCONTEXT` is modified to only include a small subset of all the `LOCALCONTEXT` within the particular iteration j .

A. Initialization

At the very first iteration, the prompt is initialized based on a set of the following inputs:

- The design platform (e.g., ASAP7).
- The circuit under consideration (e.g., AES).
- The optimization task (e.g., minimize wirelength (WL)).
- The inputs, which include design parameters (e.g., the 12 parameters such as core utilization, etc.).
- The outputs, specifying the variable sets (e.g., detailed WL) and variable sets of surrogate(s) (e.g., CTS WL).
- The exact output to optimize from the variables (e.g., $-WL$ for maximization or WL for minimization).
- The domains of the inputs, including whether they are Boolean, integers with min/max bounds, or continuous values converted to integers (e.g., converting float ranges such as 0.01–0.99 to integer ranges such as 1–99, and scaling back to original values for **PARAMETERS** generation).
- Suggested ranges for inputs.

B. Toolbox

We define three separate kinds of tools. All of these require a **Description**, a set of ideally typed **arguments**, and a return object **Return** with description and type specifications to be efficiently made

a part of LLM function-calling frameworks. We summarize tool details in Appendix F.

INSPECT tools. These tools enable quick analysis of numeric datasets by computing summary statistics, correlations, outlier indices, or performing principal component analysis. They do not consume raw data token-by-token but instead return concise analytical results that aid downstream decision-making.

OPTIMIZE tools. These tools propose new points (parameter sets) to explore in an optimization process. Each one uses a different strategy – ranging from random sampling and grid-based approaches to more sophisticated algorithms such as Bayesian optimization or genetic algorithms – to balance exploration and exploitation.

AGGLOM tools. These tools *agglomerate* (reduce or cluster) a large set of candidate solutions into a smaller or more representative subset. Methods include selecting the Pareto front for multi-objective problems, maximizing coverage or diversity, or clustering to find the most central or diverse candidates.

APPENDIX F TOOL DETAILS

INSPECT Tools

AnalyzeManifold analyzes the underlying manifold structure using PCA, TSNE, and MDS. It takes `X: np.ndarray` and an optional `config: Dict`, and returns a summary as a `Dict`.

AnalyzeLocal examines local structure using LOF and DBSCAN. It accepts `X: np.ndarray` and an optional `config: Dict`, and returns a summary `Dict`.

InspectDistribution analyzes statistical properties of input/output data. It requires `X: np.ndarray`, `Y: np.ndarray`, and optionally `Y_surrogate: np.ndarray`. The output is a summary: `Dict`.

InspectStructure inspects structural properties and gives model recommendations. Inputs include `X: np.ndarray`, `Y: np.ndarray`, and optionally `config: Dict`. It returns a summary: `Dict`.

OPTIMIZE Tools

CreateModel creates and configures a Gaussian process model. It takes `X: np.ndarray`, `y: np.ndarray`, `noise_level: float`, and `kernel_type: str`. It returns a model of type `GaussianProcessRegressor`.

CreateKernel generates a kernel from a given specification. Required inputs are `kernel_spec: str` and `input_dim: int`. The output is a GPR kernel.

ExpectedImprovement calculates the Expected Improvement (EI) acquisition function. Inputs include `mu: np.ndarray`, `std: np.ndarray`, and `y_best: float`. It returns `ei: np.ndarray`.

HandleSurrogate processes and combines true and surrogate data. It uses `X: np.ndarray`, `y: np.ndarray`, and `surrogate_values: np.ndarray`. It returns a tuple `(X, y_combined, uncertainty)`.

LatinHypercube generates Latin Hypercube samples. The inputs are `n_points: int` and `n_dims: int`. It returns samples: `np.ndarray`.

AGGLOM Tools

SelectPoints selects points based on a specified method. It accepts `X: np.ndarray`, `quality_scores: np.ndarray`, `method: str`, and `n_points: int`. It returns `selected_indices: np.ndarray`.

HybridSelect combines quality and diversity for point selection. Required arguments are `X: np.ndarray`, `quality_scores: np.ndarray`, `distance_matrix: np.ndarray`, and `n_points: int`. It returns `selected_indices: np.ndarray`.

EntropySelect uses entropy-based diversity for selection. It takes `X: np.ndarray`, `quality_scores: np.ndarray`, and `n_points: int`. It returns `selected_indices: np.ndarray`.

GraphSelect applies graph-based diversity metrics for point selection. It accepts `X: np.ndarray`, `quality_scores: np.ndarray`, and `n_points: int`. It returns `selected_indices: np.ndarray`.

CreateQualityScores computes quality scores from model predictions. Inputs include `X: np.ndarray`, `y: np.ndarray`, `model_predictions: np.ndarray`, and optionally `model_uncertainties: np.ndarray`. It returns `quality_scores: np.ndarray`.

Each of the tools used here can be implemented using standard Python packages. For instance, `scikit-learn`, `numpy` and related Python packages offer support for Gaussian processes, t-SNE modeling, and so on. By combining these existing libraries with domain-specific logic, we create a modular, maintainable toolbox that reflects the iterative exploration process a human data scientist would perform – streamlining tasks such as outlier detection, dimensionality reduction, and optimization-driven design.

APPENDIX G RESULTS WITH BETTER LLMs

Recently, Anthropic released the Claude 4 [67] class of models – Sonnet and Opus 4. Our main results use Sonnet 3.5, and hence our ongoing work seeks to rigorously quantify the benefit from more recent models.

One preliminary run on ASAP7-IBEX with the Sonnet 4 architecture, under the 12 parameter setting with tool use, produced a wirelength of **86397 μ m**, markedly below all the results produced by OR-AutoTuner or our previous ORFS-agent; this result was achieved in ≤ 100 iterations. The parameters that produced this output are:

- Clock Period: 5764 ps
- Core Utilization: 69.0 %
- TNS End Percent: 100
- Global Padding: 1
- Detail Padding: 0
- Enable DPO: 1
- Pin Layer Adjust: 0.48
- Above Layer Adjust: 0.10
- Density Margin Add-On: 0.384
- Flatten Hierarchy (HIER_SYNT): 1
- CTS Cluster Size: 28.0
- CTS Cluster Diameter: 80.0

The worst slack in this case is 1612ps, resulting in an *ECP* of 4152ps, which is worse than the baseline *ECP*. This may indicate an ability of Sonnet 4 models to find solutions that degrade QoRs outside the optimization target, which we did not observe in Sonnet 3.5 models.